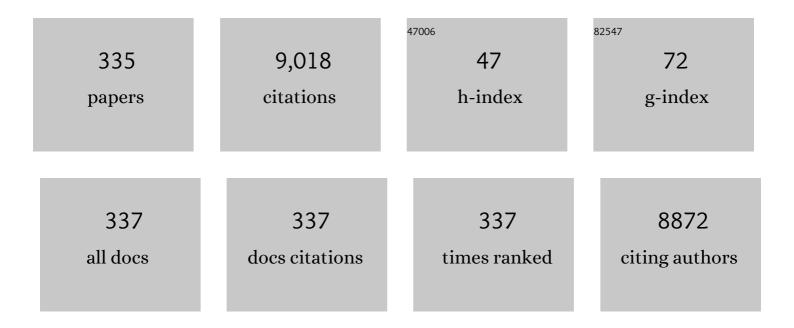
List of Publications by Year in descending order

Source: https://exaly.com/author-pdf/2126961/publications.pdf Version: 2024-02-01



#	Article	IF	CITATIONS
1	Highly Sensitive and Selective Strategy for MicroRNA Detection Based on WS <sub>2</sub> Nanosheet Mediated Fluorescence Quenching and Duplex-Specific Nuclease Signal Amplification. Analytical Chemistry, 2014, 86, 1361-1365.	6.5	348
2	MnO <sub>2</sub> -Nanosheet-Modified Upconversion Nanosystem for Sensitive Turn-On Fluorescence Detection of H <sub>2</sub> O <sub>2</sub> and Glucose in Blood. ACS Applied Materials & Interfaces, 2015, 7, 10548-10555.	8.0	315
3	Electrochemical Aptasensor Based on Proximity-Dependent Surface Hybridization Assay for Single-Step, Reusable, Sensitive Protein Detection. Journal of the American Chemical Society, 2007, 129, 15448-15449.	13.7	193
4	A novel trilinear decomposition algorithm for second-order linear calibration. Chemometrics and Intelligent Laboratory Systems, 2000, 52, 75-86.	3.5	185
5	A Targeted, Self-Delivered, and Photocontrolled Molecular Beacon for mRNA Detection in Living Cells. Journal of the American Chemical Society, 2013, 135, 12952-12955.	13.7	185
6	Graphitic Carbon Nitride Nanosheets-Based Ratiometric Fluorescent Probe for Highly Sensitive Detection of H <sub>2</sub> O <sub>2</sub> and Glucose. ACS Applied Materials & Interfaces, 2016, 8, 33439-33445.	8.0	159
7	A Highly Sensitive Target-Primed Rolling Circle Amplification (TPRCA) Method for Fluorescent <i>in Situ</i> Hybridization Detection of MicroRNA in Tumor Cells. Analytical Chemistry, 2014, 86, 1808-1815.	6.5	132
8	Alternating penalty trilinear decomposition algorithm for second-order calibration with application to interference-free analysis of excitation-emission matrix fluorescence data. Journal of Chemometrics, 2005, 19, 65-76.	1.3	122
9	A fluorescent graphitic carbon nitride nanosheet biosensor for highly sensitive, label-free detection of alkaline phosphatase. Nanoscale, 2016, 8, 4727-4732.	5.6	97
10	A dual enzyme–inorganic hybrid nanoflower incorporated microfluidic paper-based analytic device (μPAD) biosensor for sensitive visualized detection of glucose. Nanoscale, 2017, 9, 5658-5663.	5.6	95
11	Smart Photonic Crystal Hydrogel Material for Uranyl Ion Monitoring and Removal in Water. Advanced Functional Materials, 2017, 27, 1702147.	14.9	92
12	Recent developments of chemical multiway calibration methodologies with secondâ€order or higherâ€order advantages. Journal of Chemometrics, 2014, 28, 476-489.	1.3	91
13	Phospholipid-Modified Upconversion Nanoprobe for Ratiometric Fluorescence Detection and Imaging of Phospholipase D in Cell Lysate and in Living Cells. Analytical Chemistry, 2014, 86, 7119-7127.	6.5	90
14	MnO <sub>2</sub> -induced synthesis of fluorescent polydopamine nanoparticles for reduced glutathione sensing in human whole blood. Nanoscale, 2016, 8, 15604-15610.	5.6	87
15	Branched Hybridization Chain Reaction Circuit for Ultrasensitive Localizable Imaging of mRNA in Living Cells. Analytical Chemistry, 2018, 90, 1502-1505.	6.5	83
16	Efficient way to estimate the optimum number of factors for trilinear decomposition. Analytica Chimica Acta, 2001, 444, 295-307.	5.4	75
17	Interference-free determination of Sudan dyes in chilli foods using second-order calibration algorithms coupled with HPLC-DAD. Talanta, 2007, 72, 926-931.	5.5	75
18	Quantitative Spectroscopic Analysis of Heterogeneous Mixtures: The Correction of Multiplicative Effects Caused by Variations in Physical Properties of Samples. Analytical Chemistry, 2012, 84, 320-326.	6.5	75

#	Article	IF	CITATIONS
19	Highly-sensitive liquid crystal biosensor based on DNA dendrimers-mediated optical reorientation. Biosensors and Bioelectronics, 2014, 62, 84-89.	10.1	74
20	A cobalt oxyhydroxide-modified upconversion nanosystem for sensitive fluorescence sensing of ascorbic acid in human plasma. Nanoscale, 2015, 7, 13951-13957.	5.6	73
21	DNA Encapsulating Liposome Based Rolling Circle Amplification Immunoassay as a Versatile Platform for Ultrasensitive Detection of Protein. Analytical Chemistry, 2009, 81, 9664-9673.	6.5	71
22	A cobalt oxyhydroxide nanoflake-based nanoprobe for the sensitive fluorescence detection of T4 polynucleotide kinase activity and inhibition. Nanoscale, 2016, 8, 8202-8209.	5.6	71
23	A bipedal DNA nanowalker fueled by catalytic assembly for imaging of base-excision repairing in living cells. Chemical Science, 2020, 11, 10361-10366.	7.4	71
24	Electrochemical immunosensor based on Pd–Au nanoparticles supported on functionalized PDDA-MWCNT nanocomposites for aflatoxin B1 detection. Analytical Biochemistry, 2016, 494, 10-15.	2.4	70
25	Rapid identification and quantification of cheaper vegetable oil adulteration in camellia oil by using excitation-emission matrix fluorescence spectroscopy combined with chemometrics. Food Chemistry, 2019, 293, 348-357.	8.2	70
26	Melanin-Like Nanoquencher on Graphitic Carbon Nitride Nanosheets for Tyrosinase Activity and Inhibitor Assay. Analytical Chemistry, 2016, 88, 8355-8358.	6.5	67
27	A ligation-based loop-mediated isothermal amplification (ligation-LAMP) strategy for highly selective microRNA detection. Chemical Communications, 2016, 52, 12721-12724.	4.1	65
28	Activatable Two-Photon Fluorescence Nanoprobe for Bioimaging of Glutathione in Living Cells and Tissues. Analytical Chemistry, 2014, 86, 12321-12326.	6.5	64
29	A label-free electrochemical biosensor for highly sensitive and selective detection of DNA via a dual-amplified strategy. Biosensors and Bioelectronics, 2014, 54, 442-447.	10.1	64
30	Core–Shell–Shell Multifunctional Nanoplatform for Intracellular Tumor-Related mRNAs Imaging and Near-Infrared Light Triggered Photodynamic–Photothermal Synergistic Therapy. Analytical Chemistry, 2017, 89, 10321-10328.	6.5	63
31	Novel ratiometric surface-enhanced raman spectroscopy aptasensor for sensitive and reproducible sensing of Hg2+. Biosensors and Bioelectronics, 2018, 99, 646-652.	10.1	63
32	A Mediator-Free Tyrosinase Biosensor Based on ZnO Sol-Gel Matrix. Electroanalysis, 2005, 17, 1065-1070.	2.9	62
33	Double-strand DNA-templated synthesis of copper nanoclusters as novel fluorescence probe for label-free detection of biothiols. Analytical Methods, 2013, 5, 3577.	2.7	62
34	Quench-Shield Ratiometric Upconversion Luminescence Nanoplatform for Biosensing. Analytical Chemistry, 2016, 88, 1639-1646.	6.5	59
35	A highly sensitive label-free sensor for Mercury ion (Hg2+) by inhibiting thioflavin T as DNA G-quadruplexes fluorescent inducer. Talanta, 2014, 122, 85-90.	5.5	58
36	Preliminary study on the application of near infrared spectroscopy and pattern recognition methods to classify different types of apple samples. Food Chemistry, 2011, 128, 555-561.	8.2	57

#	Article	IF	CITATIONS
37	A rapid and efficient strategy for creating super-hydrophobic coatings on various material substrates. Journal of Materials Chemistry, 2008, 18, 4442.	6.7	56
38	Immobilization of Enzymes on the Nano-Au Film Modified Glassy Carbon Electrode for the Determination of Hydrogen Peroxide and Glucose. Electroanalysis, 2004, 16, 736-740.	2.9	55
39	A MgO Nanoparticles Composite Matrixâ€Based Electrochemical Biosensor for Hydrogen Peroxide with High Sensitivity. Electroanalysis, 2010, 22, 471-477.	2.9	55
40	Fast HPLC-DAD quantification of nine polyphenols in honey by using second-order calibration method based on trilinear decomposition algorithm. Food Chemistry, 2013, 138, 62-69.	8.2	54
41	Fabrication of a LRET-based upconverting hybrid nanocomposite for turn-on sensing of H <sub>2</sub> O <sub>2</sub> and glucose. Nanoscale, 2016, 8, 8939-8946.	5.6	54
42	Alternating penalty quadrilinear decomposition algorithm for an analysis of fourâ€way data arrays. Journal of Chemometrics, 2007, 21, 133-144.	1.3	53
43	Trilinear decomposition method applied to removal of three-dimensional background drift in comprehensive two-dimensional separation data. Journal of Chromatography A, 2007, 1167, 178-183.	3.7	53
44	Novel Aptasensor Platform Based on Ratiometric Surface-Enhanced Raman Spectroscopy. Analytical Chemistry, 2017, 89, 2852-2858.	6.5	53
45	Recent advances in chemical multi-way calibration with second-order or higher-order advantages: Multilinear models, algorithms, related issues and applications. TrAC - Trends in Analytical Chemistry, 2020, 130, 115954.	11.4	53
46	Fluorescence Spectral Study of Interaction of Water-soluble Metal Complexes of Schiff-base and DNA Analytical Sciences, 2001, 17, 1031-1036.	1.6	52
47	In Situ Imaging of Individual mRNA Mutation in Single Cells Using Ligation-Mediated Branched Hybridization Chain Reaction (Ligation-bHCR). Analytical Chemistry, 2017, 89, 3445-3451.	6.5	52
48	Robust principal component analysis by projection pursuit. Journal of Chemometrics, 1993, 7, 527-541.	1.3	49
49	A novel fluorescent probe for sensitive detection and imaging of hydrazine in living cells. Talanta, 2017, 162, 225-231.	5.5	49
50	Tumor-Targeted Graphitic Carbon Nitride Nanoassembly for Activatable Two-Photon Fluorescence Imaging. Analytical Chemistry, 2018, 90, 4649-4656.	6.5	49
51	Fast analysis of synthetic antioxidants in edible vegetable oil using trilinear component modeling of liquid chromatography–diode array detection data. Journal of Chromatography A, 2012, 1264, 63-71.	3.7	48
52	A sensitive electrochemical biosensor for microRNA detection based on streptavidin–gold nanoparticles and enzymatic amplification. Analytical Methods, 2014, 6, 2889-2893.	2.7	47
53	Single-Nanoparticle ICPMS DNA Assay Based on Hybridization-Chain-Reaction-Mediated Spherical Nucleic Acid Assembly. Analytical Chemistry, 2020, 92, 2379-2382.	6.5	46
54	Three-way data resolution by alternating slice-wise diagonalization (ASD) method. Journal of Chemometrics, 2000, 14, 15-36.	1.3	45

#	Article	IF	CITATIONS
55	A novel label-free fluorescence aptamer-based sensor method for cocaine detection based on isothermal circular strand-displacement amplification and graphene oxide absorption. New Journal of Chemistry, 2013, 37, 3998.	2.8	45
56	Multi-targeted interference-free determination of ten β-blockers in human urine and plasma samples by alternating trilinear decomposition algorithm-assisted liquid chromatography–mass spectrometry in full scan mode: Comparison with multiple reaction monitoring. Analytica Chimica Acta, 2014, 848, 10-24.	5.4	45
57	Determination of pesticides in vegetable samples using an acetylcholinesterase biosensor based on nanoparticles ZrO <sub>2</sub> /chitosan composite film. International Journal of Environmental Analytical Chemistry, 2005, 85, 163-175.	3.3	43
58	Activatable Fluorescence Probe via Self-Immolative Intramolecular Cyclization for Histone Deacetylase Imaging in Live Cells and Tissues. Analytical Chemistry, 2018, 90, 5534-5539.	6.5	43
59	On the self-weighted alternating trilinear decomposition algorithm?the property of being insensitive to excess factors used in calculation. Journal of Chemometrics, 2001, 15, 439-453.	1.3	41
60	Label-Free and Multiplexed Quantification of microRNAs by Mass Spectrometry Based on Duplex-Specific-Nuclease-Assisted Recycling Amplification. Analytical Chemistry, 2019, 91, 2120-2127.	6.5	41
61	Determination of the number of components in mixtures using a new approach incorporating chemical information. Journal of Chemometrics, 1999, 13, 15-30.	1.3	39
62	Simultaneous determination of umbelliferone and scopoletin in Tibetan medicine Saussurea laniceps and traditional Chinese medicine Radix angelicae pubescentis using excitation-emission matrix fluorescence coupled with second-order calibration method. Spectrochimica Acta - Part A: Molecular and Biomolecular Spectroscopy, 2017, 170, 104-110.	3.9	39
63	Programmable Self-Assembly of Protein-Scaffolded DNA Nanohydrogels for Tumor-Targeted Imaging and Therapy. Analytical Chemistry, 2019, 91, 2610-2614.	6.5	39
64	lodide-Selective PVC Membrane Electrodes Based on Five Transitional Metal Chelates ofbis-furfural-semi-o-tolidine. Analytical Letters, 1997, 30, 1455-1464.	1.8	38
65	Resolution of two-way data from spectroscopic monitoring of reaction or process systems by parallel vector analysis (PVA) and window factor analysis (WFA): inspection of the effect of mass balance, methods and simulations. Journal of Chemometrics, 2003, 17, 186-197.	1.3	38
66	Amperometric Biosensors for Glucose Based on Layerâ€by‣ayer Assembled Functionalized Carbon Nanotube and Poly (Neutral Red) Multilayer Film. Analytical Letters, 2006, 39, 1785-1799.	1.8	36
67	Simultaneous determination of phenolic antioxidants in edible vegetable oils by HPLC–FLD assisted with second-order calibration based on ATLD algorithm. Journal of Chromatography B: Analytical Technologies in the Biomedical and Life Sciences, 2014, 947-948, 32-40.	2.3	36
68	Direct quantitative analysis of aromatic amino acids in human plasma by four-way calibration using intrinsic fluorescence: Exploration of third-order advantages. Talanta, 2014, 122, 293-301.	5.5	36
69	"Light-up―Sensing of human 8-oxoguanine DNA glycosylase activity by target-induced autocatalytic DNAzyme-generated rolling circle amplification. Biosensors and Bioelectronics, 2016, 79, 679-684.	10.1	35
70	Detection of inborn errors of metabolism utilizing GC-MS urinary metabolomics coupled with a modified orthogonal partial least squares discriminant analysis. Talanta, 2017, 165, 545-552.	5.5	35
71	Sensitive inkjet printing paper-based colormetric strips for acetylcholinesterase inhibitors with indoxyl acetate substrate. Talanta, 2017, 162, 174-179.	5.5	35
72	Multivalent Self-Assembled DNA Polymer for Tumor-Targeted Delivery and Live Cell Imaging of Telomerase Activity. Analytical Chemistry, 2018, 90, 13188-13192.	6.5	35

#	Article	IF	CITATIONS
73	A Sensitive Electrochemical Immunosensor for αâ€Fetoprotein Detection with Colloidal Goldâ€Based Dentritical Enzyme Complex Amplification. Electroanalysis, 2010, 22, 244-250.	2.9	34
74	Labelâ€Free Electrochemical Biosensor of Mercury Ions Based on DNA Strand Displacement by Thymine–Hg(II)–Thymine Complex. Electroanalysis, 2010, 22, 2110-2116.	2.9	34
75	Background eliminated signal-on electrochemical aptasensing platform for highly sensitive detection of protein. Biosensors and Bioelectronics, 2015, 66, 363-369.	10.1	34
76	Label-Free Photonic Crystal-Based β-Lactamase Biosensor for β-Lactam Antibiotic and β-Lactamase Inhibitor. Analytical Chemistry, 2016, 88, 9207-9212.	6.5	34
77	Photonic crystal enhanced gold-silver nanoclusters fluorescent sensor for Hg2+ ion. Analytica Chimica Acta, 2020, 1114, 50-57.	5.4	34
78	Direct and interference-free determination of thirteen phenolic compounds in red wines using a chemometrics-assisted HPLC-DAD strategy for authentication of vintage year. Analytical Methods, 2017, 9, 3361-3374.	2.7	33
79	Internal standard-based SERS aptasensor for ultrasensitive quantitative detection of Ag+ ion. Talanta, 2018, 185, 30-36.	5.5	33
80	Interaction of Metal Complexes of Bis(salicylidene)ethylenediamine with DNA Analytical Sciences, 2000, 16, 1255-1259.	1.6	32
81	The Electrochemical Properties of Co(TPP), Tetraphenylborate Modified Glassy Carbon Electrode: Application to Dopamine and Uric Acid Analysis. Electroanalysis, 2006, 18, 440-448.	2.9	32
82	A label-free electrochemical impedance immunosensor for the sensitive detection of aflatoxin B <sub>1</sub> . Analytical Methods, 2015, 7, 2354-2359.	2.7	32
83	Label-free liquid crystal biosensor for L-histidine: A DNAzyme-based platform for small molecule assay. Biosensors and Bioelectronics, 2016, 79, 650-655.	10.1	32
84	Fast quantitative analysis of four tyrosine kinase inhibitors in different human plasma samples using three-way calibration- assisted liquid chromatography with diode array detection. Journal of Separation Science, 2015, 38, 2781-2788.	2.5	31
85	A highly selective iodide electrode based on the bis(benzoin)-semiethylenediamine complex of mercury(II) as a carrier. Fresenius' Journal of Analytical Chemistry, 1998, 360, 47-51.	1.5	30
86	Rapid and simultaneous determination of five vinca alkaloids in Catharanthus roseus and human serum using trilinear component modeling of liquid chromatography–diode array detection data. Journal of Chromatography B: Analytical Technologies in the Biomedical and Life Sciences, 2016, 1026, 114-123.	2.3	30
87	DNA-stabilized silver nanoclusters with guanine-enhanced fluorescence as a novel indicator for enzymatic detection of cholesterol. Analytical Methods, 2013, 5, 2182.	2.7	29
88	Mass Spectrometry Based Ultrasensitive DNA Methylation Profiling Using Target Fragmentation Assay. Analytical Chemistry, 2016, 88, 1083-1087.	6.5	29
89	Mitochondrial-targeted near-infrared fluorescence probe for selective detection of fluoride ions in living cells. Talanta, 2019, 204, 655-662.	5.5	29
90	Analysis of PAHs in air-borne particulates in Hong Kong City by heuristic evolving latent projections. Science in China Series B: Chemistry, 1998, 41, 21-29.	0.8	28

#	Article	IF	CITATIONS
91	A PARAFAC algorithm using penalty diagonalization error (PDE) for three-way data array resolution. Analyst, The, 2000, 125, 2303-2310.	3.5	28
92	Chemometrics-enhanced liquid chromatography-full scan-mass spectrometry for interference-free analysis of multi-class mycotoxins in complex cereal samples. Chemometrics and Intelligent Laboratory Systems, 2017, 160, 125-138.	3.5	28
93	CoOOH-induced synthesis of fluorescent polydopamine nanoparticles for the detection ofÂascorbic acid. Analytical Methods, 2017, 9, 5518-5524.	2.7	28
94	A novel DNAzyme-based colorimetric assay for the detection of hOGG1 activity with lambda exonuclease cleavage. Analytical Methods, 2013, 5, 164-168.	2.7	27
95	Chemometrics-assisted high performance liquid chromatography-diode array detection strategy to solve varying interfering patterns from different chromatographic columns and sample matrices for beverage analysis. Journal of Chromatography A, 2016, 1435, 75-84.	3.7	27
96	Mitochondrion-Targeting, Environment-Sensitive Red Fluorescent Probe for Highly Sensitive Detection and Imaging of Vicinal Dithiol-Containing Proteins. Analytical Chemistry, 2017, 89, 11203-11207.	6.5	27
97	<i>In vivo</i> mRNA imaging based on tripartite DNA probe mediated catalyzed hairpin assembly. Chemical Communications, 2020, 56, 8782-8785.	4.1	27
98	Network training and architecture optimization by a recursive approach and a modified genetic algorithm. Journal of Chemometrics, 1996, 10, 253-267.	1.3	26
99	Alternating coupled vectors resolution (ACOVER) method for trilinear analysis of three-way data. Journal of Chemometrics, 1999, 13, 557-578.	1.3	26
100	Pseudo alternating least squares algorithm for trilinear decomposition. Journal of Chemometrics, 2001, 15, 149-167.	1.3	26
101	A Sequenceâ€Selective Electrochemical DNA Biosensor Based on HRPâ€Labeled Probe for Colorectal Cancer DNA Detection. Analytical Letters, 2008, 41, 24-35.	1.8	26
102	An efficient fluorescence turn-on probe for Al3+ based on aggregation-induced emission. Analytical Methods, 2013, 5, 3909.	2.7	26
103	Simultaneous determination of eight flavonoids in propolis using chemometrics-assisted high performance liquid chromatography-diode array detection. Journal of Chromatography B: Analytical Technologies in the Biomedical and Life Sciences, 2014, 962, 59-67.	2.3	26
104	Light-up RNA aptamer enabled label-free protein detection <i>via</i> a proximity induced transcription assay. Chemical Communications, 2018, 54, 8877-8880.	4.1	26
105	Activatable CRISPR Transcriptional Circuits Generate Functional RNA for mRNA Sensing and Silencing. Angewandte Chemie - International Edition, 2020, 59, 18599-18604.	13.8	26
106	DNAzyme cascade circuits in highly integrated DNA nanomachines for sensitive microRNAs imaging in living cells. Biosensors and Bioelectronics, 2021, 177, 112976.	10.1	26
107	Bimetallic gold–silver nanocluster fluorescent probes for Cr( <scp>iii</scp> ) and Cr( <scp>vi</scp> ). Analytical Methods, 2016, 8, 7237-7241.	2.7	25
108	Aggregation-Induced Emission-Based Fluorescence Probe for Fast and Sensitive Imaging of Formaldehyde in Living Cells. ACS Omega, 2018, 3, 14417-14422.	3.5	25

#	Article	IF	CITATIONS
109	Target-based metabolomics for fast and sensitive quantification of eight small molecules in human urine using HPLC-DAD and chemometrics tools resolving of highly overlapping peaks. Talanta, 2019, 201, 174-184.	5.5	25
110	A novel ethacrynic acid sensor based on a lanthanide porphyrin complex in a PVC matrix. Analyst, The, 2000, 125, 867-870.	3.5	24
111	Dry film method with ytterbium as the internal standard for near infrared spectroscopic plasma glucose assay coupled with boosting support vector regression. Journal of Chemometrics, 2006, 20, 13-21.	1.3	24
112	A Reagentless Tyrosinase Biosensor Based on 1,6-Hexanedithiol and Nano-Au Self-Assembled Monolayers. Electroanalysis, 2006, 18, 1572-1577.	2.9	24
113	Chemometrics-enhanced high performance liquid chromatography-diode array detection strategy for simultaneous determination of eight co-eluted compounds in ten kinds of Chinese teas using second-order calibration method based on alternating trilinear decomposition algorithm. Journal of Chromatography A, 2014, 1364, 151-162.	3.7	24
114	Chemometrics-enhanced full scan mode of liquid chromatography–mass spectrometry for the simultaneous determination of six co-eluted sulfonylurea-type oral antidiabetic agents in complex samples. Chemometrics and Intelligent Laboratory Systems, 2016, 155, 62-72.	3.5	24
115	Picric acid sensitive optode based on a fluorescence carrier covalently bound to membrane. Analyst, The, 2001, 126, 349-352.	3.5	23
116	Interference-free determination of abscisic acid and gibberellin in plant samples using excitation-emission matrix fluorescence based on oxidation derivatization coupled with second-order calibration methods. Analytical Methods, 2009, 1, 115.	2.7	23
117	A novel method to handle Rayleigh scattering in three-way excitation-emission fluorescence data. Analytical Methods, 2012, 4, 3987.	2.7	23
118	A label free exonuclease III-aided fluorescence assay for adenosine triphosphate based on graphene oxide and ligation reaction. New Journal of Chemistry, 2013, 37, 927.	2.8	23
119	An electrochemical assay of polynucleotide kinase activity based on streptavidin–gold nanoparticles and enzymatic amplification. RSC Advances, 2013, 3, 18128.	3.6	23
120	Quantitative detection of captopril in tablet and blood plasma samples by the combination of surfaceâ€enhanced Raman spectroscopy with multiplicative effects model. Journal of Raman Spectroscopy, 2015, 46, 605-609.	2.5	23
121	Nucleic acid amplification-based methods for microRNA detection. Analytical Methods, 2015, 7, 2258-2263.	2.7	23
122	Sensitive fluorescence sensing of T4 polynucleotide kinase activity and inhibition based on DNA/polydopamine nanospheres platform. Talanta, 2018, 180, 271-276.	5.5	23
123	Mitochondrion-Targeting Fluorescence Probe via Reduction Induced Charge Transfer for Fast Methionine Sulfoxide Reductases Imaging. Analytical Chemistry, 2019, 91, 5489-5493.	6.5	23
124	Rapid and Sensitive Detection of Multi-Class Food Additives in Beverages for Quality Control by Using HPLC-DAD and Chemometrics Methods. Food Analytical Methods, 2019, 12, 381-393.	2.6	23
125	Excitation-emission matrix fluorescence spectroscopy coupled with multi-way chemometric techniques for characterization and classification of Chinese lager beers. Food Chemistry, 2021, 342, 128235.	8.2	23
126	Highly Sensitive and Specific Mass Spectrometric Platform for miRNA Detection Based on the Multiple-Metal-Nanoparticle Tagging Strategy. Analytical Chemistry, 2021, 93, 5839-5848.	6.5	23

#	Article	IF	CITATIONS
127	Fast identification of the geographical origin of Gastrodia elata using excitation-emission matrix fluorescence and chemometric methods. Spectrochimica Acta - Part A: Molecular and Biomolecular Spectroscopy, 2021, 258, 119798.	3.9	23
128	Simultaneous determination of aromatic amino acids in different systems using three-way calibration based on the PARAFAC-ALS algorithm coupled with EEM fluorescence: exploration of second-order advantages. Analytical Methods, 2014, 6, 6358-6368.	2.7	22
129	Plasmon Coupling Enhanced Raman Scattering Nanobeacon for Single-Step, Ultrasensitive Detection of Cholera Toxin. Analytical Chemistry, 2016, 88, 7447-7452.	6.5	22
130	Rapid and interference-free analysis of nine B-group vitamins in energy drinks using trilinear component modeling of liquid chromatography-mass spectrometry data. Talanta, 2018, 180, 108-119.	5.5	22
131	Highly specific and sensitive detection of microRNAs by tandem signal amplification based on duplex-specific nuclease and strand displacement. Chemical Communications, 2019, 55, 14210-14213.	4.1	22
132	A novel electrochemical immunosensor for ochratoxin A with hapten immobilization on thionine/gold nanoparticle modified glassy carbon electrode. Analytical Methods, 2013, 5, 1481.	2.7	21
133	A novel fourth-order calibration method based on alternating quinquelinear decomposition algorithm for processing high performance liquid chromatography–diode array detection– kinetic-pH data of naptalam hydrolysis. Analytica Chimica Acta, 2015, 861, 12-24.	5.4	21
134	Cyclodextrin supramolecular inclusion-enhanced pyrene excimer switching for time-resolved fluorescence detection of biothiols in serum. Biosensors and Bioelectronics, 2015, 68, 253-258.	10.1	21
135	Quantitative fluorescence kinetic analysis of NADH and FAD in human plasma using three- and four-way calibration methods capable of providing the second-order advantage. Analytica Chimica Acta, 2016, 910, 36-44.	5.4	21
136	A novel mitochondrial-targeting near-infrared fluorescent probe for imaging Î <sup>3</sup> -glutamyl transpeptidase activity in living cells. Analyst, The, 2018, 143, 5530-5535.	3.5	21
137	A simple method for direct modeling of second-order liquid chromatographic data with retention time shifts and holding the second-order advantage. Journal of Chromatography A, 2019, 1605, 360360.	3.7	21
138	An intramolecular charge transfer and excited state intramolecular proton transfer based fluorescent probe for highly selective detection and imaging of formaldehyde in living cells. Analyst, The, 2019, 144, 6922-6927.	3.5	21
139	Cascade Circuits on Self-Assembled DNA Polymers for Targeted RNA Imaging In Vivo. Analytical Chemistry, 2020, 92, 15953-15958.	6.5	21
140	Renewable amperometric immunosensor based on paraffin–graphite–transferrin antiserum biocomposite for transferrin assay. Analyst, The, 2000, 125, 1595-1599.	3.5	20
141	Label-Free Detection of DNA Hybridization Based on MnO2Nanoparticles. Analytical Letters, 2009, 42, 3046-3057.	1.8	20
142	Colorimetric Sensing of Adenosine Based on Aptamer Binding Inducing Gold Nanoparticle Aggregation. Chinese Journal of Chemistry, 2009, 27, 1855-1859.	4.9	20
143	Setschenow Constant Prediction Based on the IEF-PCM Calculations. Industrial & Engineering Chemistry Research, 2013, 52, 11182-11188.	3.7	20
144	Improving the quantitative accuracy of surface-enhanced Raman spectroscopy by the combination of microfluidics with a multiplicative effects model. Analytical Methods, 2014, 6, 2363-2370.	2.7	20

#	Article	IF	CITATIONS
145	A study on the differential strategy of some iterative trilinear decomposition algorithms: PARAFACâ€ALS, ATLD, SWATLD, and APTLD. Journal of Chemometrics, 2015, 29, 179-192.	1.3	20
146	A novel, label-free fluorescent aptasensor for cocaine detection based on a G-quadruplex and ruthenium polypyridyl complex molecular light switch. Analytical Methods, 2016, 8, 3740-3746.	2.7	20
147	Surface Enhanced Laser Desorption Ionization of Phospholipids on Gold Nanoparticles for Mass Spectrometric Immunoassay. Analytical Chemistry, 2016, 88, 9881-9884.	6.5	20
148	A chemometrics-assisted excitation–emission matrix fluorescence method for simultaneous determination of arbutin and hydroquinone in cosmetic products. Analytical Methods, 2016, 8, 4941-4948.	2.7	20
149	A label-free and highly sensitive strategy for uracil-DNA glycosylase activity detection based on stem-loop primer-mediated exponential amplification (SPEA). Analytica Chimica Acta, 2017, 991, 127-132.	5.4	20
150	Recombinant Fusion Streptavidin as a Scaffold for DNA Nanotetrads for Nucleic Acid Delivery and Telomerase Activity Imaging in Living Cells. Analytical Chemistry, 2019, 91, 9361-9365.	6.5	20
151	Construction and Research of Multiple Stimuli-Responsive 2D Photonic Crystal DNA Hydrogel Sensing Platform with Double-Network Structure and Signal Self-Expression. Analytical Chemistry, 2022, 94, 5530-5537.	6.5	20
152	A non-linear mapping-based generalized backpropagation network for unsupervised learning. Journal of Chemometrics, 1996, 10, 241-252.	1.3	19
153	Electrochemical Aptasensor Based on Proximityâ€Dependent Surface Hybridization Assay for Protein Detection. Electroanalysis, 2009, 21, 1327-1333.	2.9	19
154	Self-weighted alternating normalized residue fitting algorithm with application to quantitative analysis of excitation-emission matrix fluorescence data. Analytical Methods, 2010, 2, 1918.	2.7	19
155	New function of exonuclease and highly sensitive label-free colorimetric DNA detection. Biosensors and Bioelectronics, 2016, 77, 879-885.	10.1	19
156	Rapid, simultaneous and interference-free determination of three rhodamine dyes illegally added into chilli samples using excitation-emission matrix fluorescence coupled with second-order calibration method. Spectrochimica Acta - Part A: Molecular and Biomolecular Spectroscopy, 2018, 204, 141-149.	3.9	19
157	Three-dimensional DNA nanostructures for dual-color microRNA imaging in living cells <i>via</i> hybridization chain reaction. Chemical Communications, 2020, 56, 6668-6671.	4.1	19
158	A flexible and novel strategy of alternating trilinear decomposition method coupled with two-dimensional linear discriminant analysis for three-way chemical data analysis: Characterization and classification. Analytica Chimica Acta, 2018, 1021, 28-40.	5.4	18
159	DNAzyme activated protein-scaffolded CRISPR–Cas9 nanoassembly for genome editing. Chemical Communications, 2019, 55, 6511-6514.	4.1	18
160	Simultaneous imaging of lysosomal and mitochondrial viscosity during mitophagy using molecular rotors with dual-color emission. Chemical Communications, 2020, 56, 7797-7800.	4.1	18
161	Neutral carrier membrane electrode based on binuclear metalloporphyrin. Fresenius' Journal of Analytical Chemistry, 1995, 351, 484-488.	1.5	17
162	A new thirdâ€order calibration method with application for analysis of fourâ€way data arrays. Journal of Chemometrics, 2011, 25, 408-429.	1.3	17

#	Article	IF	CITATIONS
163	Algorithm combination strategy to obtain the secondâ€order advantage: simultaneous determination of target analytes in plasma using threeâ€dimensional fluorescence spectroscopy. Journal of Chemometrics, 2012, 26, 197-208.	1.3	17
164	Development of a highly sensitive sensing platform for T4 polynucleotide kinase phosphatase and its inhibitors based on WS <sub>2</sub> nanosheets. Analytical Methods, 2014, 6, 7212-7217.	2.7	17
165	A flexible trilinear decomposition algorithm for three-way calibration based on the trilinear component model and a theoretical extension of the algorithm to the multilinear component model. Analytica Chimica Acta, 2015, 878, 63-77.	5.4	17
166	Interference-free spectrofluorometric quantification of aristolochic acid I and aristololactam I in five Chinese herbal medicines using chemical derivatization enhancement and second-order calibration methods. Spectrochimica Acta - Part A: Molecular and Biomolecular Spectroscopy, 2017, 175, 229-238.	3.9	17
167	Quantification of Cadmium in Rice by Surface-enhanced Raman Spectroscopy Based on a Ratiometric Indicator and Conical Holed Enhancing Substrates. Analytical Sciences, 2018, 34, 1405-1410.	1.6	17
168	A single promoter system co-expressing RNA sensor with fluorescent proteins for quantitative mRNA imaging in living tumor cells. Chemical Science, 2019, 10, 4828-4833.	7.4	17
169	Simultaneously quantifying intracellular FAD and FMN using a novel strategy of intrinsic fluorescence four-way calibration. Talanta, 2019, 197, 105-112.	5.5	17
170	Development of large Stokes shift, near-infrared fluorescence probe for rapid and bioorthogonal imaging of nitroxyl (HNO) in living cells. Talanta, 2019, 193, 152-160.	5.5	17
171	Amperometric Biosensor for Glucose Based on Electropolymerized Tetraaminophthalo-Cyanatocobalt(II) and Phenol Films. Analytical Letters, 1997, 30, 647-662.	1.8	16
172	Simultaneous determination of pre-emergence herbicides in environmental samples using HPLC-DAD combined with second-order calibration based on self-weighted alternating trilinear decomposition algorithm. Analytical Methods, 2012, 4, 685.	2.7	16
173	Measuring estriol and estrone simultaneously in liquid cosmetic samples using second-order calibration coupled with excitation–emission matrix fluorescence based on region selection. Analytical Methods, 2012, 4, 222-229.	2.7	16
174	Sensitive and selective electrochemical DNA sensor for the analysis of cancer-related single nucleotide polymorphism. New Journal of Chemistry, 2014, 38, 4711-4715.	2.8	16
175	An aptasensor based on cobalt oxyhydroxide nanosheets for the detection of thrombin. Analytical Methods, 2016, 8, 7199-7203.	2.7	16
176	Simultaneous detection of multiple inherited metabolic diseases using GC-MS urinary metabolomics by chemometrics multi-class classification strategies. Talanta, 2018, 186, 489-496.	5.5	16
177	Proximity-induced hybridization chain assembly with small-molecule linked DNA for single-step amplified detection of antibodies. Chemical Communications, 2019, 55, 4387-4390.	4.1	16
178	Simultaneous and fast determination of bisphenol A and diphenyl carbonate in polycarbonate plastics by using excitation-emission matrix fluorescence couples with second-order calibration method. Spectrochimica Acta - Part A: Molecular and Biomolecular Spectroscopy, 2019, 216, 283-289.	3.9	16
179	Single-step, high-specificity detection of single nucleotide mutation by primer-activatable loop-mediated isothermal amplification (PA-LAMP). Analytica Chimica Acta, 2019, 1050, 132-138.	5.4	16
180	Single-Nanoparticle ICP-MS for Sensitive Detection of Uracil-DNA Glycosylase Activity. Analytical Chemistry, 2021, 93, 8381-8385.	6.5	16

#	Article	IF	CITATIONS
181	Second-Order Standard Addition Method Based on Alternating Trilinear Decomposition Analytical Sciences, 2000, 16, 217-220.	1.6	15
182	Amplified fluorescence detection of T4 polynucleotide kinase activity and inhibition via a coupled λ exonuclease reaction and exonuclease III-aided trigger DNA recycling. Analytical Methods, 2014, 6, 6009.	2.7	15
183	Chemometrics-assisted liquid chromatography-full scan mass spectrometry for simultaneous determination of multi-class estrogens in infant milk powder. Analytical Methods, 2018, 10, 1459-1471.	2.7	15
184	Chemometrics-assisted HPLC-DAD as a rapid and interference-free strategy for simultaneous determination of 17 polyphenols in raw propolis. Analytical Methods, 2018, 10, 5577-5588.	2.7	15
185	Rapid and simultaneous determination of three fluoroquinolones in animal-derived foods using excitation-emission matrix fluorescence coupled with second-order calibration method. Spectrochimica Acta - Part A: Molecular and Biomolecular Spectroscopy, 2020, 224, 117458.	3.9	15
186	A tumour mRNA-triggered nanoassembly for enhanced fluorescence imaging-guided photodynamic therapy. Nanoscale, 2020, 12, 8727-8731.	5.6	15
187	Comparison of three chemometric methods for processing HPLC-DAD data with time shifts: Simultaneous determination of ten molecular targeted anti-tumor drugs in different biological samples. Talanta, 2021, 224, 121798.	5.5	15
188	Coupled Vectors Resolution Method for Chemometric Calibration with Three-Way Data. Analytical Chemistry, 1999, 71, 4254-4262.	6.5	14
189	A ratiometric fluorescent probe for zinc ions based on the quinoline fluorophore. International Journal of Environmental Analytical Chemistry, 2011, 91, 74-86.	3.3	14
190	Conformational switching of G-quadruplexes as a label-free platform for the fluorescence detection of Ag <sup>+</sup> and biothiols. Analytical Methods, 2016, 8, 311-315.	2.7	14
191	Multiplex protein pattern unmixing using a non-linear variable-weighted support vector machine as optimized by a particle swarm optimization algorithm. Talanta, 2016, 147, 609-614.	5.5	14
192	Chemometricsâ€assisted liquid chromatography with full scan mass spectrometry for the interferenceâ€free determination of glucocorticoids illegally added to face masks. Journal of Separation Science, 2018, 41, 3527-3537.	2.5	14
193	Geographical origin traceability of traditional Chinese medicine Atractylodes macrocephala Koidz. by using multi-way fluorescence fingerprint and chemometric methods. Spectrochimica Acta - Part A: Molecular and Biomolecular Spectroscopy, 2022, 269, 120737.	3.9	14
194	Discrimination of Vapours of Alcohols and Beverage Samples Using Piezoelectric Crystal Sensor Array. Analytical Letters, 1995, 28, 451-466.	1.8	13
195	Electropolymerization of 1-naphthylamine and the structure of the polymer film. Mikrochimica Acta, 1995, 117, 145-152.	5.0	13
196	Sequential number-theoretic optimization (SNTO) method applied to chemical quantitative analysis. Journal of Chemometrics, 1997, 11, 267-281.	1.3	13
197	Chemical rank estimation for excitation—emission matrices using a morphological approach. Journal of Chemometrics, 1998, 12, 95-104.	1.3	13
198	Robust linear discriminant analysis for chemical pattern recognition. Journal of Chemometrics, 1999, 13, 3-13.	1.3	13

#	Article	IF	CITATIONS
199	Nano-ZnO/Chitosan Composite Film Modified Electrode for Voltammetric Detection of DNA Hybridization. Analytical Letters, 2008, 41, 1083-1095.	1.8	13
200	A Thirdâ€Generation Hydrogen Peroxide Biosensor Based on Horseradish Peroxidase Immobilized in Carbon Nanotubes/ SBAâ€45 Film. Electroanalysis, 2011, 23, 2415-2420.	2.9	13
201	Discovery of the unique self-assembly behavior of terminal suckers-contained dsDNA onto GNP and novel "light-up―colorimetric assay of nucleic acids. Biosensors and Bioelectronics, 2015, 64, 292-299.	10.1	13
202	Graphene oxide–peptide nanoassembly as a general approach for monitoring the activity of histone deacetylases. Analyst, The, 2016, 141, 3989-3992.	3.5	13
203	Fast and simultaneous determination of 12 polyphenols in apple peel and pulp by using chemometricsâ€assisted highâ€performance liquid chromatography with diode array detection. Journal of Separation Science, 2017, 40, 1651-1659.	2.5	13
204	Cyclodextrin supramolecular inclusion-enhanced pyrene excimer switching for highly selective detection of RNase H. Analytica Chimica Acta, 2019, 1088, 137-143.	5.4	13
205	Coupling bootstrap with synergy self-organizing map-based orthogonal partial least squares discriminant analysis: Stable metabolic biomarker selection for inherited metabolic diseases. Talanta, 2020, 219, 121370.	5.5	13
206	Ultrasensitive detection of protein biomarkers by MALDI-TOF mass spectrometry based on ZnFe2O4 nanoparticles and mass tagging signal amplification. Talanta, 2021, 224, 121848.	5.5	13
207	Salicylate-Sensitive Membrane Electrode Based on Copper(II) Tetraaza[14]annulene Macrocyclic Complex. Analytical Letters, 1998, 31, 1965-1977.	1.8	12
208	Reagentless Aptamer Based Impedance Biosensor for Monitoring Adenosine. Electroanalysis, 2009, 21, 1781-1785.	2.9	12
209	Chemometrics-assisted determination of amiloride and triamterene in biological fluids with overlapped peaks and unknown interferences. Bioanalysis, 2015, 7, 1685-1697.	1.5	12
210	A new label-free and turn-on fluorescence probe for hydrogen peroxide and glucose detection based on DNA–silver nanoclusters. Analytical Methods, 2015, 7, 7989-7994.	2.7	12
211	Quantitative analysis of hormones in cosmetics by LC-MS/MS combined with an advanced calibration model. Analytical Methods, 2015, 7, 6804-6809.	2.7	12
212	Simultaneous and interference-free determination of eleven non-steroidal anti-inflammatory drugs illegally added into Chinese patent drugs using chemometrics-assisted HPLC-DAD strategy. Science China Chemistry, 2018, 61, 739-749.	8.2	12
213	A novel ratiometric fluorescent sensing method based on MnO2 nanosheet for sensitive detection of alkaline phosphatase in serum. Talanta, 2020, 209, 120528.	5.5	12
214	DNA-Programmed plasmonic ELISA for the ultrasensitive detection of protein biomarkers. Analyst, The, 2020, 145, 4860-4866.	3.5	12
215	Simple Multivariate Calibration Method with an Appropriate Number of Principal Components Using Singular Value Decomposition and Cross-Validation Procedure Analytical Sciences, 1994, 10, 875-880.	1.6	11
216	A sensitive nicotine sensor based on molecularly imprinted electropolymer of o-aminophenol. Frontiers of Chemistry in China: Selected Publications From Chinese Universities, 2006, 1, 183-187.	0.4	11

#	Article	IF	CITATIONS
217	Quantitative analysis of fluphenazine hydrochloride in human urine using excitation-emission matrix fluorescence based on oxidation derivatization and combined with second-order calibration methods. Analytical Methods, 2010, 2, 1069.	2.7	11
218	A combined theoretical and experimental study for the chiral discrimination of naproxen enantiomers by molecular modeling and second-order standard addition method. Analytical Methods, 2013, 5, 710.	2.7	11
219	A turn-on upconversion fluorescence resonance energy transfer biosensor for ultrasensitive endonuclease detection. Analytical Methods, 2015, 7, 7474-7479.	2.7	11
220	Solving signal instability to maintain the second-order advantage in the resolution and determination of multi-analytes in complex systems by modeling liquid chromatography–mass spectrometry data using alternating trilinear decomposition method assisted with piecewise direct standardization. Journal of Chromatography A, 2015, 1407, 157-168.	3.7	11
221	Desorption corona beam ionisation (DCBI) mass spectrometry for in-situ analysis of adsorbed phenol in cigarette acetate fiber filter. Talanta, 2015, 131, 499-504.	5.5	11
222	Interference-free analysis of aflatoxin B <sub>1</sub> and G <sub>1</sub> in various foodstuffs using trilinear component modeling of excitation–emission matrix fluorescence data enhanced through photochemical derivatization. RSC Advances, 2016, 6, 25850-25863.	3.6	11
223	Phosphorylation-induced formation of a cytochrome c-peptide complex: a novel fluorescent sensing platform for protein kinase assay. Chemical Communications, 2016, 52, 776-779.	4.1	11
224	Small molecule-linked programmable DNA for washing-free imaging of cell surface biomarkers. Talanta, 2018, 190, 429-435.	5.5	11
225	Simultaneous and rapid screening and determination of twelve azo dyes illegally added into food products by using chemometrics-assisted HPLC-DAD strategy. Microchemical Journal, 2021, 171, 106775.	4.5	11
226	An Amperometric Immunosensor for the Newcastle Disease Antibody Assay. Analytical Letters, 2003, 36, 287-302.	1.8	10
227	Studying the uptake of aniline vapor by active alumina through in-line monitoring a differential adsorption bed with near-infrared diffuse reflectance spectroscopy. Adsorption, 2009, 15, 23-29.	3.0	10
228	Automatic configuration of optimized sample-weighted least-squares support vector machine by particle swarm optimization for multivariate spectral analysis. Analytical Methods, 2010, 2, 282.	2.7	10
229	Graphene–hemin hybrid nanosheets as a label-free colorimetric platform for DNA and small molecule assays. RSC Advances, 2014, 4, 64252-64257.	3.6	10
230	An aggregated perylene-based broad-spectrum, efficient and label-free quencher for multiplexed fluorescent bioassays. Biosensors and Bioelectronics, 2014, 58, 320-325.	10.1	10
231	A simple and highly sensitive DNAzyme-based assay for nicotinamide adenine dinucleotide by ligase-mediated inhibition of strand displacement amplification. Analytica Chimica Acta, 2014, 844, 70-74.	5.4	10
232	Silver nanocluster-lightened hybridization chain reaction. RSC Advances, 2016, 6, 57502-57506.	3.6	10
233	Exploiting second-order advantage from mathematically modeled liquid chromatography–mass spectrometry data for simultaneous determination of polyphenols in Chinese propolis. Microchemical Journal, 2020, 157, 105003.	4.5	10
234	An Optic-Fiber Sensor for Metronidazole Based on the Fluorescence Quenching of a Copolymer Bound Flavone Derivative Analytical Sciences, 1998, 14, 547-551.	1.6	9

#	Article	lF	CITATIONS
235	A Fiber Optode for p -Nitrophenol Based on Covalently Bound 9-Allylaminoacridine. Mikrochimica Acta, 2001, 136, 73-78.	5.0	9
236	A Sensitive Electrochemical Biosensor for Detection of Histone Deacetylase Activity Using an Acetylated Peptide. Electroanalysis, 2012, 24, 2365-2370.	2.9	9
237	A novel molecular logic system based on lead-induced substitution of potassium from a G-quadruplex as a fluorescent lead sensor. Analytical Methods, 2013, 5, 5597.	2.7	9
238	Highly Sensitive Fluorometric Assay Method for Acetylcholinesterase Inhibitor Based on Nile Redâ€Adsorbed Gold Nanoparticles. Chinese Journal of Chemistry, 2013, 31, 1072-1078.	4.9	9
239	Label-free and sensitive detection of micrococcal nuclease activity using DNA-scaffolded silver nanoclusters as a fluorescence indicator. Analytical Methods, 2014, 6, 4090.	2.7	9
240	Generalized multiple internal standard method for quantitative liquid chromatography mass spectrometry. Journal of Chromatography A, 2016, 1445, 112-117.	3.7	9
241	Graphene oxide based DNA nanoswitches as a programmable pH-responsive biosensor. Analytical Methods, 2016, 8, 6982-6985.	2.7	9
242	An activatable fluorescent probe with an ultrafast response and large Stokes shift for live cell bioimaging of hypochlorous acid. RSC Advances, 2016, 6, 107910-107915.	3.6	9
243	Determination of benzo[a]pyrene in cigarette mainstream smoke by using mid-infrared spectroscopy associated with a novel chemometric algorithm. Analytica Chimica Acta, 2016, 902, 43-49.	5.4	9
244	Ratiometric sensors with selective fluorescence enhancement effects based on photonic crystals for the determination of acetylcholinesterase and its inhibitor. Journal of Materials Chemistry B, 2020, 8, 11001-11009.	5.8	9
245	Quantitative analysis of carbaryl and thiabendazole in complex matrices using excitation-emission fluorescence matrices with second-order calibration methods. Spectrochimica Acta - Part A: Molecular and Biomolecular Spectroscopy, 2022, 264, 120267.	3.9	9
246	CAPACITIVE IMMUNOSENSOR FOR THE DETERMINATION OFSCHISTOSOMA JAPONICUMANTIGEN. Analytical Letters, 2002, 35, 1919-1930.	1.8	8
247	Self-assembled monolayers of inositol hexaphosphate on the roughened surface of an iron electrode: investigation by surface-enhanced Raman scattering spectroscopy. Journal of Raman Spectroscopy, 2005, 36, 824-828.	2.5	8
248	Amperometric Biosensors Based on Platinum Nanowires. Analytical Letters, 2007, 40, 875-886.	1.8	8
249	Quantitative Structure–Activity Relationship Studies for the Binding Affinities of Imidazobenzodiazepines for the α6 Benzodiazepine Receptor Isoform Utilizing Optimized Blockwise Variable Combination by Particle Swarm Optimization for Partial Least Squares Modeling. QSAR and Combinatorial Science. 2007. 26. 92-101.	1.4	8
250	Synthesis and Characterization of Poly(toluidine blue) Nanowires and Their Application in Amperometric Biosensors. Electroanalysis, 2009, 21, 1152-1158.	2.9	8
251	Surface-enhanced Raman spectroscopy based on conical holed enhancing substrates. Analytica Chimica Acta, 2015, 887, 45-50.	5.4	8
252	A novel logic gate based on liquid-crystals responding to the DNA conformational transition. Analyst, The, 2016, 141, 2870-2873.	3.5	8

#	Article	IF	CITATIONS
253	Development of an electrochemical aptasensor for thrombin based on aptamer/Pd–AuNPs/HRP conjugates. Analytical Methods, 2016, 8, 2150-2155.	2.7	8
254	Application of gold–silver nanocluster based fluorescent sensors for determination of acetylcholinesterase activity and its inhibitor. Materials Research Express, 2018, 5, 065027.	1,6	8
255	Generalized ratiometric fluorescence nanosensors based on carbon dots and an advanced chemometric model. Talanta, 2019, 192, 233-240.	5.5	8
256	Detection of microRNAs by the combination of Exonuclease-III assisted target recycling amplification and repeated-fishing strategy. Analytica Chimica Acta, 2020, 1131, 1-8.	5.4	8
257	Three efficient chemometrics assisted fluorimetric detection methods for interference-free, rapid, and simultaneous determination of ibrutinib and pralatrexate in various complicated biological fluids. Spectrochimica Acta - Part A: Molecular and Biomolecular Spectroscopy, 2021, 252, 119419.	3.9	8
258	Control of Liquid Crystal Microarray Optical Signals Using a Microspectral Mode Based on Photonic Crystal Structures. Analytical Chemistry, 2021, 93, 11887-11895.	6.5	8
259	Rapid determination of sulfamethoxazole and trimethoprim illegally added to health products using excitation–emission matrix fluorescence coupled with the second-order calibration method. Analytical Methods, 2021, 13, 5075-5084.	2.7	8
260	Single Molecule-Level Detection via Liposome-Based Signal Amplification Mass Spectrometry Counting Assay. Analytical Chemistry, 2022, 94, 6120-6129.	6.5	8
261	Non-linear discriminant feature extraction using generalized back-propagation network. Journal of Chemometrics, 1996, 10, 281-294.	1.3	7
262	A Novel Potentiometric Sensor for Thiocyanate Based on an Amide‣inked Manganese Diporphyrin Xanthene. Electroanalysis, 2008, 20, 1769-1774.	2.9	7
263	Homogeneous label-free fluorescent assay of small molecule-protein interactions using protein binding-inhibited transcription nanomachine. Science China Chemistry, 2011, 54, 1277-1283.	8.2	7
264	Second-order calibration applied to quantification of two active components of Schisandra chinensis in complex matrix. Journal of Pharmaceutical Analysis, 2012, 2, 241-248.	5.3	7
265	Acetylcholinesterase liquid crystal biosensor for identification of AChE inhibitors by a reactivator. Science China Chemistry, 2014, 57, 1589-1595.	8.2	7
266	Interaction of epicatechin with bovine serum albumin using fluorescence quenching combined with chemometrics. Science China Chemistry, 2014, 57, 748-754.	8.2	7
267	An alternating coupled two-unequal residual functions algorithm for second-order calibration. Analytical Methods, 2014, 6, 6322.	2.7	7
268	A novel electrochemical immunosensor based on dual signal amplification of gold nanoparticles and telomerase extension reaction. Analytical Methods, 2014, 6, 2221-2226.	2.7	7
269	Novel calibration model maintenance strategy for solving the signal instability in quantitative liquid chromatography–mass spectrometry. Journal of Chromatography A, 2014, 1338, 44-50.	3.7	7
270	Adaptive wavelet packet transform for support vector machine modeling as globally optimized by particle swarm optimization algorithm. Analytical Methods, 2015, 7, 5108-5113.	2.7	7

#	Article	IF	CITATIONS
271	A dual-amplification fluorescent sensing platform for ultrasensitive assay of nuclease and ATP based on rolling circle replication and exonuclease III-aided recycling. RSC Advances, 2015, 5, 75055-75061.	3.6	7
272	Duplex-specific nuclease-mediated target recycling amplification for fluorescence detection of microRNA. Analytical Methods, 2019, 11, 200-204.	2.7	7
273	Exploration advantages of data combination and partition: First chemometric analysis of liquid chromatography–mass spectrometry data in full scan mode with quadruple fragmentor voltages. Analytica Chimica Acta, 2020, 1110, 158-168.	5.4	7
274	A New Optical Chemical Sensor Based on Benzoxazole and Its Application to the Determination of Ethacrynic Acid. Analytical Letters, 1997, 30, 221-233.	1.8	6
275	Bismetalloporphyrin Complexes as Ionic Carriers for a Salicylate-Sensitive Electrode Analytical Sciences, 2000, 16, 1285-1289.	1.6	6
276	PORPHYRIN DIMER AS NEUTRAL IONOPHORE FOR A BERBERINE-SENSITIVE POTENTIOMETRIC SENSOR. Analytical Letters, 2001, 34, 2035-2046.	1.8	6
277	Adsorption of purpald SAMs on silver and gold electrodes: a Raman mapping study. Journal of Raman Spectroscopy, 2007, 38, 295-300.	2.5	6
278	Homogeneous DNA Detection Based on Fluorescence Quenching by Nanoparticles in Singleâ€step Format: Targetâ€Induced Configuration Transform. Chinese Journal of Chemistry, 2009, 27, 523-528.	4.9	6
279	Nonlinear Multivariate Calibration of Shelf Life of Preserved Eggs (Pidan) by Near Infrared Spectroscopy: Stacked Least Squares Support Vector Machine with Ensemble Preprocessing. Journal of Spectroscopy, 2013, 2013, 1-7.	1.3	6
280	A novel label-free biosensor based on self-assembled aptamer/GO architecture for sensitive detection of biomolecules. Analytical Methods, 2015, 7, 5606-5610.	2.7	6
281	Quantitative generalized ratiometric fluorescence spectroscopy for turbid media based on probe encapsulated by biologically localized embedding. Analytica Chimica Acta, 2016, 921, 38-45.	5.4	6
282	Loop-mediated isothermal amplification (LAMP): real-time methods for the detection of the survivin gene in cancer cells. Analytical Methods, 2016, 8, 6277-6283.	2.7	6
283	A novel algorithm for second-order calibration of three-way data in fluorescence assays of multiple breast cancer-related DNAs. Talanta, 2019, 195, 433-440.	5.5	6
284	Label-free microRNA detection through analyzing the length distribution pattern of the residual fragments of probe DNA produced during exonuclease III assisted signal amplification by mass spectrometry. Talanta, 2021, 231, 122414.	5.5	6
285	Constrained background bilinearization with a generalized simulated annealing algorithm. Journal of Chemometrics, 1993, 7, 369-379.	1.3	5
286	Maximum sum of binary-coded residuals (MASBR) regression as a robust procedure for treatment of spectral data. Journal of Chemometrics, 1995, 9, 373-387.	1.3	5
287	Bismetalloporphyrin-based ISE sensitive to fluoroborate. Analyst, The, 2000, 125, 2285-2288.	3.5	5
288	Aminobenzothiazole Schiff Base as a Fluorescence Carrier for Sensor Preparation and Furazolidone Assay. Analytical Letters, 2003, 36, 2609-2622.	1.8	5

#	Article	IF	CITATIONS
289	An Aptamer-Based Competitive Fluorescence Quenching Assay for IgE. Analytical Letters, 2011, 44, 1301-1309.	1.8	5
290	Rapid Determination of Costunolide and Dehydrocostuslactone in Human Plasma Sample and Chinese Patent Medicine Xiang Sha Yang Wei Capsule Using HPLCâ€DAD Coupled with Secondâ€order Calibration. Chinese Journal of Chemistry, 2012, 30, 1137-1143.	4.9	5
291	HPLC-DAD data coupled with second-order calibration method applied to food analysis: Simultaneous determination of six benzoylurea insecticides in various fruit samples by selecting time region of chromatogram. Science China Chemistry, 2013, 56, 1641-1650.	8.2	5
292	Determination of Lead(II) by a Nitrocellulose Membrane Fluorescent Biosensor Based on G-Quadruplex Conformational Changes. Analytical Letters, 2014, 47, 2341-2349.	1.8	5
293	Two new algorithms for resolution of two-way data. Journal of Chemometrics, 1996, 10, 63-76.	1.3	4
294	A Simple and Sensitive Piezoelectric Immunosensor for Cholera Toxin Based on GM1â€Incorporated Liposome Agglutination. Chinese Journal of Chemistry, 2010, 28, 1678-1684.	4.9	4
295	Terminal Protection of Small Molecule-Linked DNA for Small Molecule–Protein Interaction Assays. International Journal of Molecular Sciences, 2014, 15, 5221-5232.	4.1	4
296	Efficient pattern unmixing of multiplex proteins based on variable weighting of texture descriptors. Analytical Methods, 2016, 8, 8188-8195.	2.7	4
297	A Novel Biosensor Based on Terminal Protection and Fluorescent Copper Nanoparticles for Detecting Potassium Ion. Analytical Sciences, 2017, 33, 1369-1374.	1.6	4
298	A chemometric comparison of different models in fluorescence analysis of dabigatran etexilate and dabigatran. Spectrochimica Acta - Part A: Molecular and Biomolecular Spectroscopy, 2021, 246, 118988.	3.9	4
299	Piecewise direct standardization assisted with second-order calibration methods to solve signal instability in high-performance liquid chromatography-diode array detection systems. Journal of Chromatography A, 2022, 1667, 462851.	3.7	4
300	Partial induced reorientation of 5CB in a liquid crystal microarray and a signal-on sensing assay for the detection of aflatoxin B1. Chemical Communications, 2022, 58, 5009-5012.	4.1	4
301	Matrix-assisted laser desorption/ionization time-of-flight mass spectrometry combined with chemometrics to identify the origin of Chinese medicinal materials. RSC Advances, 2022, 12, 16886-16892.	3.6	4
302	Relationship between the Potentiometric Response Characteristics of Primary Amine Electrodes Based on Synthetic Polyether Derivatives of 1,10-Phenanthroline and Membrane Transport Characteristics Analytical Sciences, 1994, 10, 413-418.	1.6	3
303	Detection of linear substructures in calibration model by robust approach: Maximum sum of binary-coded residuals (MASBR) regression. Journal of Chemometrics, 1996, 10, 295-307.	1.3	3
304	A New Fluorescence Optical-Fiber Sensor for Colchicine Analytical Sciences, 1997, 13, 447-451.	1.6	3
305	An Optical-Fiber Sensor for Colchicine Using Photo-Polymerized N-Vinylcarbazole. Mikrochimica Acta, 2003, 142, 225-230.	5.0	3
306	Aspects of recent developments in analytical chemometrics. Science in China Series B: Chemistry, 2006, 49, 193-203.	0.8	3

#	Article	IF	CITATIONS
307	Simultaneous Determination of Dextromethorphan and Quinidine Contents in Biological Fluid Samples Using Excitation-Emission Matrix Fluorescence Coupled with Second-Order Calibration Methods. Analytical Letters, 2010, 43, 2739-2750.	1.8	3
308	Quantitative study of state switching in proteins using a single probe combined with trilinear decomposition. New Journal of Chemistry, 2014, 38, 2422-2427.	2.8	3
309	Mass spectrometry based trinucleotide repeat sequence detection using target fragment assay. Analytical Methods, 2016, 8, 5039-5044.	2.7	3
310	A novel calibration strategy based on background correction for quantitative circular dichroism spectroscopy. Talanta, 2017, 174, 320-324.	5.5	3
311	Novel Sensitive Fluorometric Determination of Exonuclease I Using Polydopamine Nanospheres. Analytical Letters, 2018, 51, 998-1012.	1.8	3
312	Quantitation of cobalt in Chinese tea by surfaceâ€enhanced Raman spectroscopy in combination with the spectral shape deformation quantitative theory. Journal of Raman Spectroscopy, 2019, 50, 322-329.	2.5	3
313	Fluoroimmunosensing System Using Ferulic Acid as the Substrate for the Determination of Transferrin. Analytical Letters, 2003, 36, 3035-3049.	1.8	2
314	Iridium Oxide Filmâ€Enhanced Impedance Immunosensor for Rapid Detection of Carcinoembyronic Antigen. Chinese Journal of Chemistry, 2007, 25, 1288-1293.	4.9	2
315	A Ligation Triggered Label-Free Fluorescent Assay for Adenosine-Triphosphate Based on Nicking Endonuclease Signal Amplification and Ligand Responsive G-Quadruplex Formation. Analytical Letters, 2013, 46, 1097-1107.	1.8	2
316	Gold Nanoparticle Based Fluorescence Resonance Energy Transfer Immunoassay for the Detection of the Histone Deacetylase Activity using a Fluorescent Peptide Probe. Analytical Letters, 2013, 46, 2029-2039.	1.8	2
317	Prediction of the <i>Q</i> - <i>e</i> parameters from transition state structures. Polymer Engineering and Science, 2013, 53, n/a-n/a.	3.1	2
318	Magnetic separation–enrichment-mediated signal amplification for a simple and sensitive fluorometric assay of biotin. Analytical Methods, 2014, 6, 2091-2095.	2.7	2
319	Fluorescence amplification detection via terminal protection of small molecule–protein interactions. RSC Advances, 2015, 5, 107179-107184.	3.6	2
320	An assumption-free quantitative polymerase chain reaction method with internal standard. Talanta, 2020, 220, 121405.	5.5	2
321	Activatable CRISPR Transcriptional Circuits Generate Functional RNA for mRNA Sensing and Silencing. Angewandte Chemie, 2020, 132, 18758-18763.	2.0	2
322	Simultaneous determination of nine tyrosine kinase inhibitors in three complex biological matrices by using highâ€performance liquid chromatography–diode array detection combined with a secondâ€order calibration method. Journal of Separation Science, 2021, 44, 3914-3923.	2.5	2
323	Quantification of miRNAs by mass spectrometry based on DNase I-assisted amplification with the aid of a chemometric model. Chemometrics and Intelligent Laboratory Systems, 2022, 227, 104603.	3.5	2
324	Multivariate Calibration in Chemometrics: the Robust Approach Analytical Sciences, 1994, 10, 149-153.	1.6	1

#	Article	IF	CITATIONS
325	Direct determination of reserpine in urine using excitation-emission fluorescence combined with three-way chemometric calibration methodologies. Frontiers of Chemistry in China: Selected Publications From Chinese Universities, 2008, 3, 224-228.	0.4	1
326	Electrochemical Detection of <i>Schistosoma Japonicum</i> Antibody Using Biocatalytic Deposition. Analytical Letters, 2008, 41, 2237-2250.	1.8	1
327	Chemometrics-assisted excitation-emission fluorescence spectroscopy for simultaneous determination of ethoxyquin and tert-butylhydroquinone in biological fluid samples. Science China Chemistry, 2013, 56, 664-671.	8.2	1
328	Chemometrics in China. Journal of Chemometrics, 2018, 32, e3094.	1.3	1
329	Label-free and sensitive microRNA detection method based on the locked nucleic acid assisted fishing amplification strategy. Talanta, 2022, 240, 123169.	5.5	1
330	Data fusion of synchronous fluorescence and surface enhanced Raman scattering spectroscopies for geographical origin traceability of Atractylodes macrocephala Koidz. Spectroscopy Letters, 2022, 55, 290-301.	1.0	1
331	Potentiometric Sensor Based on Modified BLM on Rigid Support. Analytical Letters, 1994, 27, 2249-2259.	1.8	0
332	Immunoaffinity Column Based on Electrostatic Self-Assembly for Flow Immunoassay. Analytical Letters, 2003, 36, 1131-1145.	1.8	0
333	Using Sub-Band Reconstruction in Wavelet Space and Fourier Transform to Extract Local Features from Analytical Signals Exactly and Straightforwardly. Analytical Letters, 2010, 43, 1019-1032.	1.8	0
334	Quantification of enantiomers by mass spectrometry based on chemical derivatization and spectral shape deformation quantitative theory. Journal of Mass Spectrometry, 2019, 54, 250-257.	1.6	0
335	Boronate carbon nanoparticles featuring efficient FRET for activatable two-photon fluorescence imaging of sialic acid surface-abundant tumor cells. Analyst, The, 2021, 146, 5567-5573.	3.5	Ο